Development of polarimeter for gamma-ray bursts onboard the Solar-Powered Sail mission

Daisuke Yonetoku[a], Toshio Murakami[a], Hiroki Masui[a], Hironobu Kodaira[a], Yuka Aoyama[a], Shuichi Gunji[b], Fuyuki Tokanai[b] and Tatehiro Mihara[c]

[a]Kanazawa University, Kakuma, Kanazawa, Ishikawa, Japan;
[b]Yamagata University, 1-4-12, Kojirakawa, Yamagata, Yamagata, Japan;
[c]RIKEN, 2-1, Hirosawa, Wako, Saitama, Japan

ABSTRACT

The solar powered sail spacecraft using a huge sail is a next Japanese engineering verification satellite planned to launch in 2012. It has a hybrid propulsion system with ion engines and a huge solar sail panel of 50 m in diameter. Based on the present mission plan, it will take about 6 years to cruise to Jupiter via Earth swing-bys and 5 more years to reach the Jovian L4 Trojan asteroids. During its cruising phase, we plan to mount a gamma-ray burst (GRB) detector with polarization detection capability which also works as one of the interplanetary network (IPN) to determine the GRB positions. The emission mechanism of GRB is thought to be the synchrotron radiation from the relativistic outflows. If the emission mechanism of GRBs is really synchrotron radiation, the emitted gamma-rays should be strongly polarized. The detection principle is the anisotropy of the Compton scattering. The Compton-scattered gamma-ray photons show the strongly biased distribution toward the vertical direction against the oscillating electric field vector. The design concept of our detector is simple but carefully avoid a fake modulation. The plastic scintillator in one Compton-length as the scattering body is placed at the center, and 12 CsI scintillators are allocated around it. To avoid a fake modulation through the satellite body scattering, these detectors work in coincidence mode. The coincidence also helps to reduce the particle background. We will use the VA-TA ASIC and FPGA as the analog readout and the digital event processing, respectively, to make the detector weight of almost 2.0 kg. In this paper, we introduce the solar sail mission and show the overview of gamma-ray polarimeter.

Keywords: satellite, gamma-ray burst, polarization

1. INTRODUCTION

Gamma-Ray Bursts (hereafter GRBs) are the most energetic explosion in the universe and most of all occur at the cosmological distance beyond the redshift of $z > 1$. At the brightest case, the isotropic luminosity reaches 10^{54} erg s^{-1}. Although a lot of physical informations about GRBs are revealed after the discovery of afterglows,[3] we have little knowledge about their emission mechanism. Theoretically, the prompt emissions and the following afterglows are thought to be generated by the synchrotron radiation. The electrons are accelerated by the strong relativistic shocks, and the strong magnetic field above 10^4 Gauss may be generated within the short time interval of prompt phase. In that case, the polarization degree of emitted photons is expected to be very strong (e.g. max 70 %). There was an earlier report of measurement of GRB's polarization,[2] but not conclusive. Therefore, the direct measurement of the polarization degree of the prompt emission is a key to probe their emission mechanism.

Recently several types of X-ray and gamma-ray polarimeter have been developed based on the principle of photon–electron interaction. Using the gas chamber with the imaging spectrometer, polarization of soft X-ray is detected by the track of moving electron generated by the photo-electric absorption. Bragg reflection is also useful to measure the polarization of monochromatic X-ray. This concept has been done by the OSO-8 satellite in 1970s.[11] However, within the energy band of typical GRB photon such as 50–300 keV, the cross-section of the Compton scattering dominates one of photo-electric absorption for the light element material. Therefore,

Further author information: (Send correspondence to Daisuke Yonetoku)
D.Y.: E-mail: yonetoku@astro.s.kanazawa-u.ac.jp

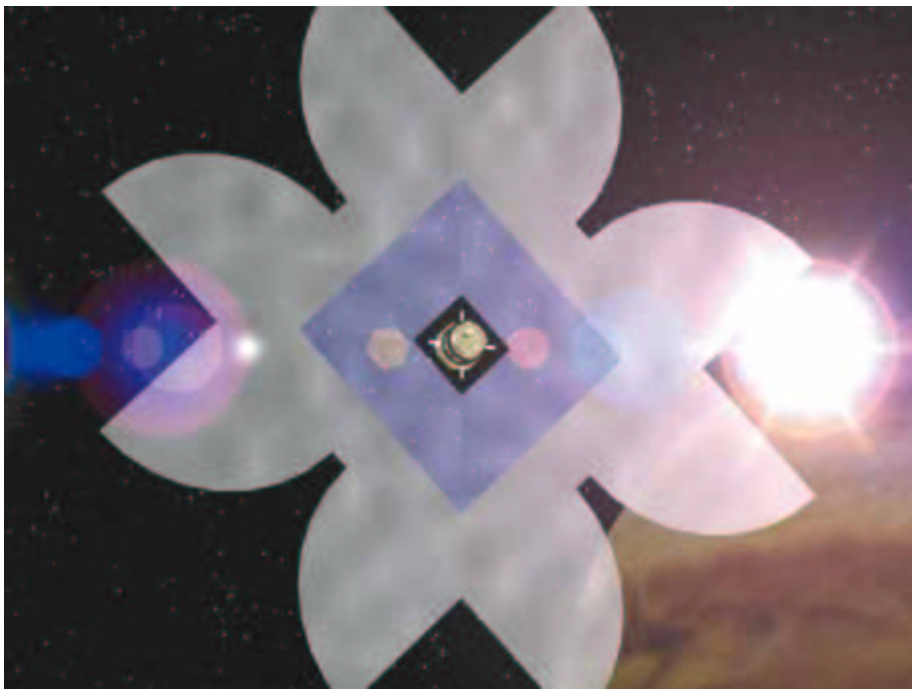

Figure 1. The concept of the solar powered sail satellite. The spacecraft expand the huge polyimide membrane with 50 m in diameter which translates the radiation pressure from the sun to the thrust of the spacecraft (from ISAS/JAXA Home Page:[13]).

it is the best to use the non-isotropic angular distribution of the Compton scattered photons. Several types of polarization detectors using this principle are developing. For example, polarization gamma-ray observer (PoGO) composed as hexagonal well-type scintillator arrays with the phoswitch technologies,[9] octagonal scintillators,[10] and matrix layout with multi-anode photomultiplier tubes,[14,5,6] and so on. Almost all of them are instruments with narrow field of view to observe steady X-ray and gamma-ray sources, such as the Crab nebula, pulsar, black hole candidate, and active galactic nuclei. Since we can never expect when and where GRBs will occur, our gamma-ray polarimeter have to cover the wide field of view. In this paper, we introduce the solar powered sail mission and our polarimeter to measure the polarization degree of prompt GRBs.

2. SOLAR POWERED SAIL AND DESIGN OF POLARIMETER FOR GRBS

The solar powered sail spacecraft is a next Japanese engineering verification spacecraft planned to launch in 2012. It has a hybrid propulsion system with ion engines and a 7.5 micron polyimide membrane of 50 m in diameter as shown in figure 1. Reflecting the photons from the sun, this sail translates their radiation pressure to the thrust of the spacecraft. This satellite rotates with the angular speed of 1 rpm to keep spreading the sail with the centrifugal forces. The purpose of this mission is to cruise to Jupiter and the Jovian L4 Trojan asteroids with the propulsion by photon reflection. As the spacecraft flies by Jupiter, a small probe will be released and inserted to a polar orbit around Jupiter in order to make simultaneous observation of the Jovian magnetosphere and solar wind interaction with the atmosphere (aurora) in the polar regions of the planet. For substantiate experiment, ISAS/JAXA launched a small rocket S-310-34 containing the small solar sail of 10 m in diameter on August 9, 2004, and it was successfully expanded. During its cruising phase toward Jupiter, we plan to measure the polarization of GRBs. We also determine the precious position of GRBs using the interplanetary network (IPN). In the following sections, we introduce a design of our gamma-ray polarimeter, and its capability estimated by the numerical simulations.

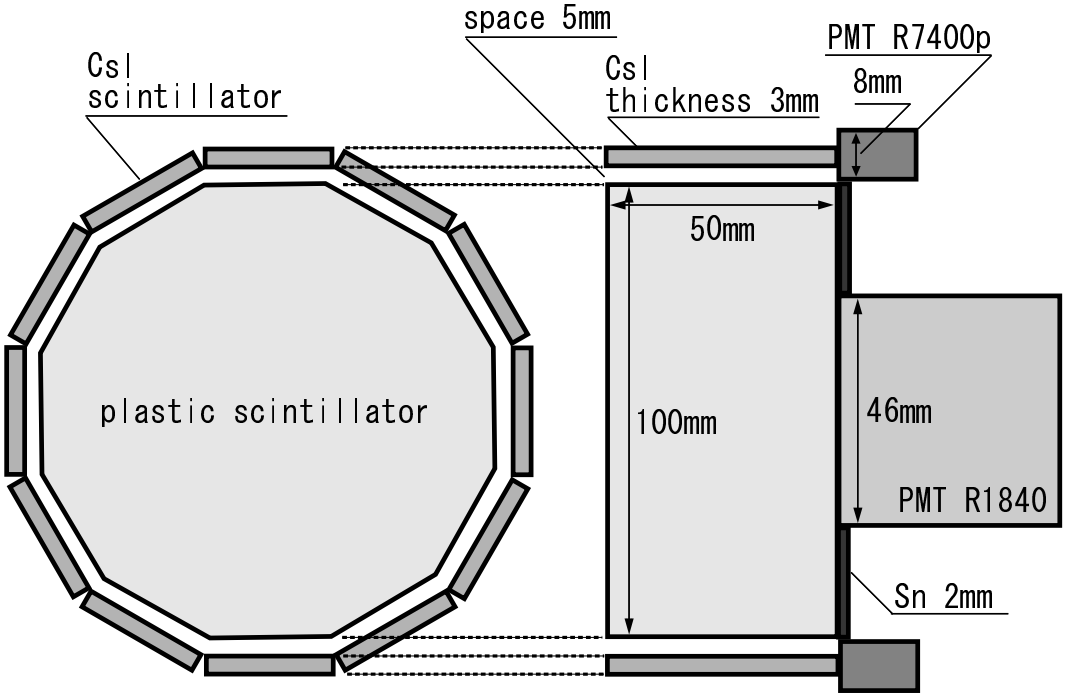

Figure 2. A schematic view of the GRB polarimeter. A central dodecagonal plastic scintillator works a gamma-ray scatterer, and the angular distribution of scattered photon is measured by the surrounding 12 CsI scintillators.

2.1. Design of Gamma-Ray Polarimeter

Assuming the non-relativistic case, for instance, the cross section of the Compton effect is due to the Klein-Nishina formula;

$$\frac{d\sigma}{d\Omega} = r_0^2(1 - \sin^2\theta\cos^2\phi). \tag{1}$$

Here, r_0 is a classical electron radius, and θ and ϕ denote altitude and azimuth angle measured from the incident photon propagation vector, respectively. In the case of 100 % polarization, the amplitude of the modulation is proportional to the function of $\sin^2\phi$ in the $\theta = \pi/2$ plane. If we obtain this modulation curve from the astronomical phenomena, it is equivalent to the direct measurement of the polarization degree.

In figure 2, we show the basic concept of our gamma-ray polarimeter. A dodecagonal plastic scintillator with the photo-multiplier tube (e.g. R1840[7]) is attached at the center, and twelve CsI scintillators with PMT (e.g. R7400p[7]) are set around it. Each scintillator is wholly polished and is covered by ESR reflection sheets. The central plastic works as the Compton scatterer, and the angular distribution of scattered photons coinciding with the plastic scintillation are measured by side CsI scintillators with the angular resolution of 30 degree.

We designed the depth of plastic as 5 cm because it satisfies one Thomson length to scatter 100 keV photons effectively. Since the scattered photons should escape from the plastic and reach CsI, its radius also should be shorter than one Thomson length. Since the CsI scintillators have to stop the scattered photons with high efficiency, we set their thickness as 3 mm whose stooping power is 88 % for 100 keV photon. These CsI counters can detect the prompt GRBs outside of the field of view, and play a role of the IPN detector together with the other satellite, e.g. GLAST, works in the same era.

In figure 3, we show both couples of scintillator and PMT. Assuming the Compton effect of incoming 60 keV photon, the energy deposit of the recoil electrons is only 6.3 keV. Therefore we provide the energy threshold of plastic scintillator as 7 keV at least. Using the detector configuration shown in figure 3, we measured the lower

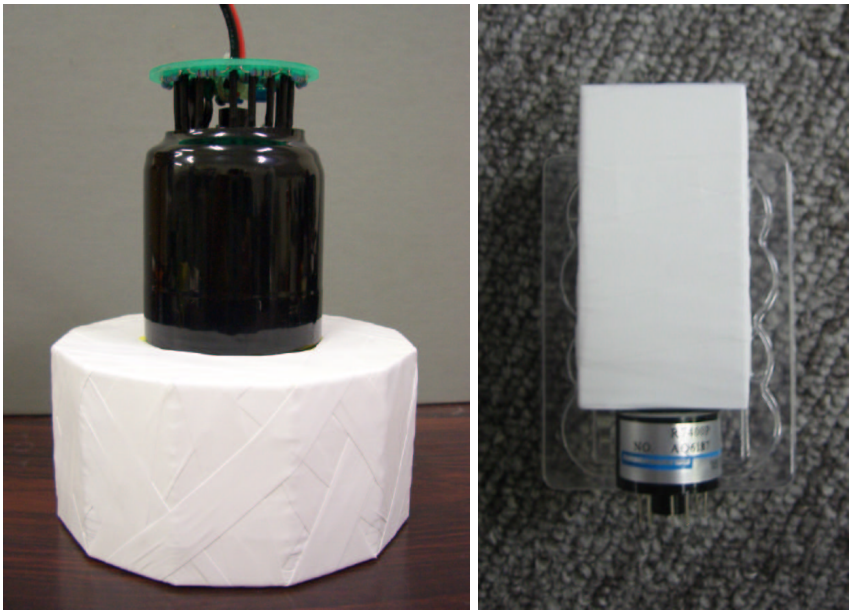

Figure 3. The left and right panel show the plastic scintillator with PMT (R1840) and the CsI with PMT (R7400p), respectively. Both scintillators are wrapped with the ESR reflectors.

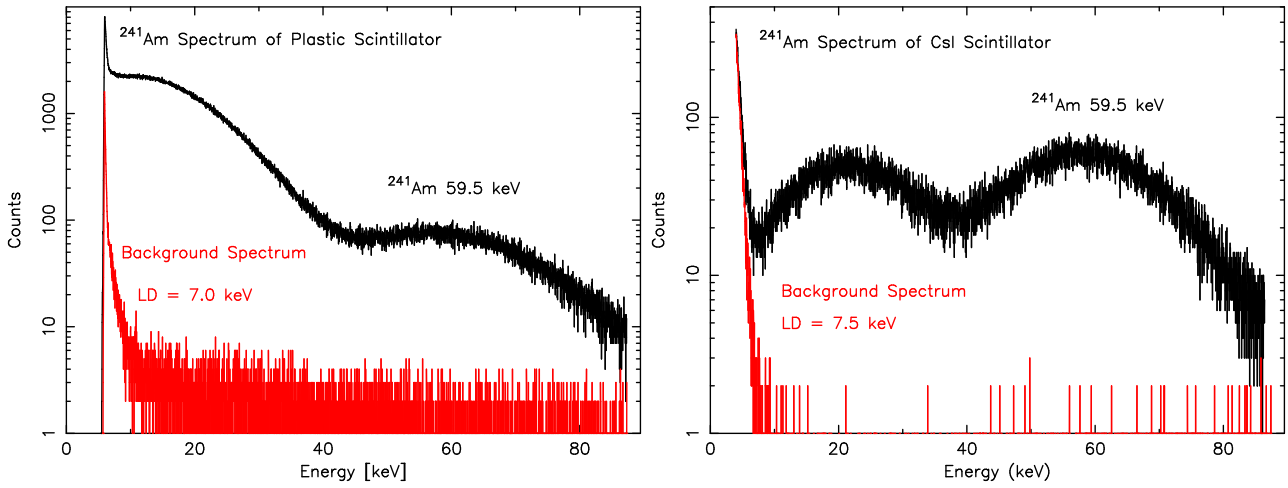

Figure 4. The left and right panels show the energy spectrum of the plastic and CsI scintillator, respectively. For both of experiments, we use the couple of scintillator and PMT as shown in figure 2. These signals are read by the charge sensitive amplifier CS515-3 and the ARTEC570 shaping amplifier.

discriminate (LD) level for each scintillator. Then we used the charge sensitive amplifier of CS515-3[1] and the shaping amplifier of ARTEC 570 with the time constant of 0.5 μs. In figure 4, we show two ^{241}Am spectra. For the plastic and CsI, LD = 7.0 keV and 7.5 keV are achieved, respectively. This fact means our polarimeter has the efficiency to measure the gamma-ray polarization for incoming photons above 60 keV. Although the several shapes of polarimeters such as hexagon or octagon, are independently developed, the geometrical symmetry of our detector is much higher than others. There is a large advantage to reduce the fake modulation without any rotation of instruments.

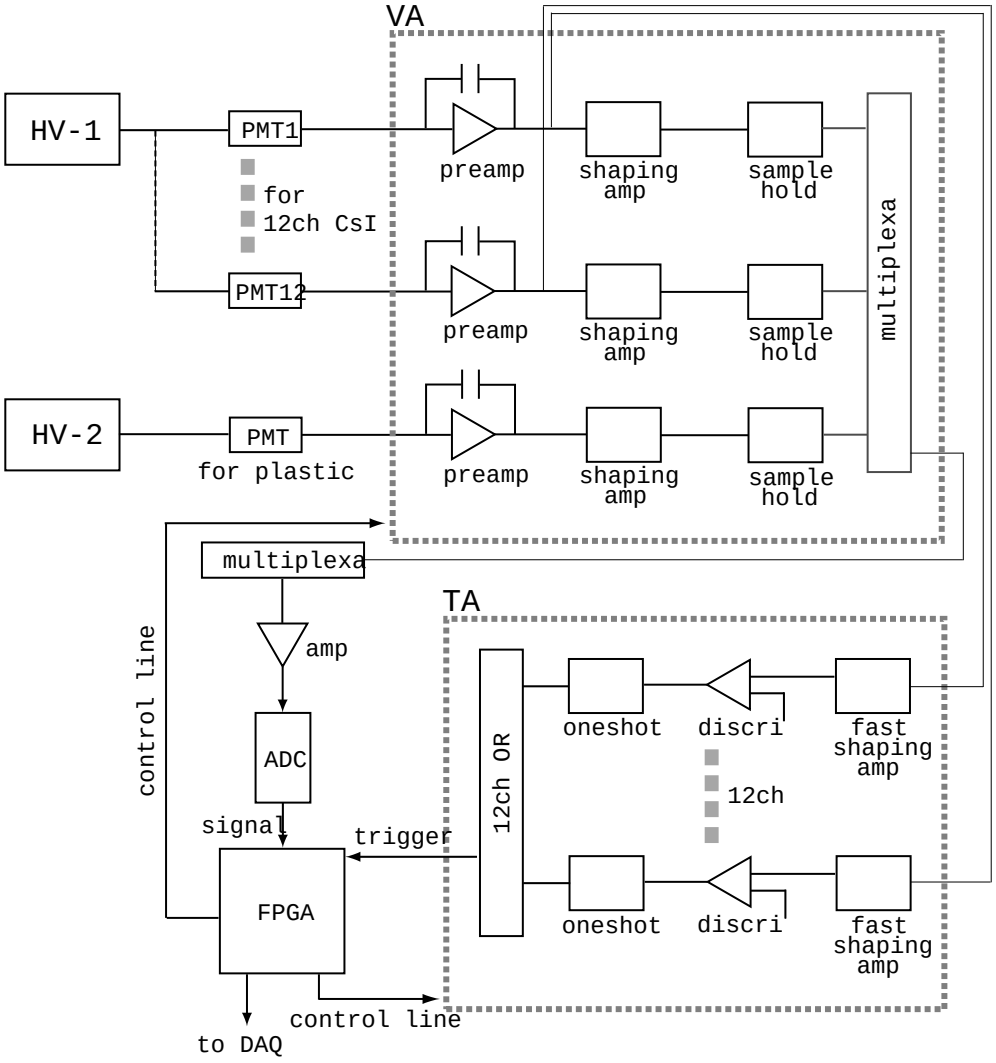

Figure 5. Flow chart of the readout circuit. The analog output from 13 PMTs are dealt with the VA–TA ASIC. The general readout stream, such as preamplifier, shaping amplifier and the sample hold, is worked in the VA-chip. The TA-chip generates the trigger output with the pulse hight discriminator. Triggered by the TA output, the following FPGA read the A/D values of all channels and reset the VA-chip. The FPGA also play a role of command interfaces.

2.2. Analog and Digital Readout

Our polarimeter has 13 analog outputs (1 plastic and 12 CsI scintillators). We would like to prepare the analog and digital circuits as light as possible because the weight limitation is $\sim$ 2 kg. Therefore we plan to use so called VA–TA ASIC and FPGA to deal with analog and digital signals, respectively. In figure 5, we show a flow chart of the readout circuit. The VA–chip works as preamplifier, shaping amplifier and sample hold for parallel inputs of 32 channels and TA–chip works pulse hight discriminator. Triggered by any PMT output, all analog pulse hight are converted to 12-bit digital signals with A/D converter controlled by the multiplexer. The data download rate from the solar sail to the ground-based antenna is very restricted compared with the near orbit satellites. Thus we plan to make a histogram of angular distribution by the FPGA aboard the solar sail. The FPGA also works as the command interface among the VA–TA, the satellite and the human operators.

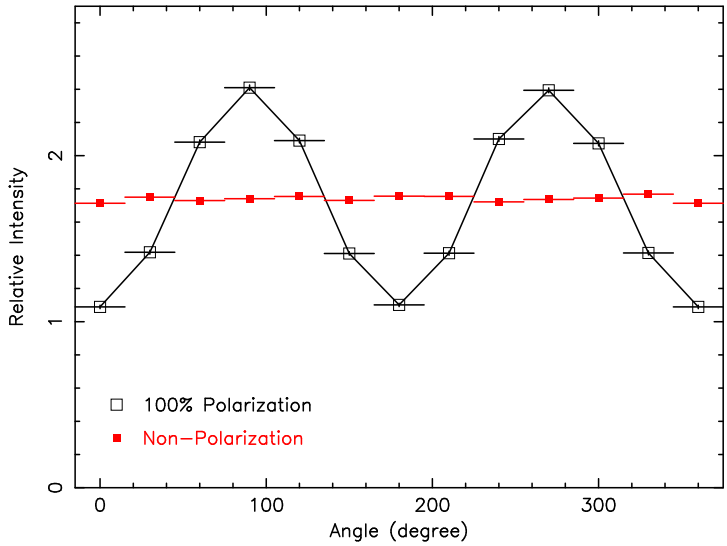

Figure 6. Modulation curves for the monochrome 100 keV gamma-ray photons estimated with the *EGS* simulation. Two cases of incoming photons with 100 % and 0 % polarization are plotted at once. For the 100 % polarization (large amplitude curve), we estimate the modulation factor of 0.39. On the other hand, for the non-polarization case (almost constant), the fake modulation caused by the geometrical effect is kept under 1 %.

3. DETECTOR CAPABILITY ESTIMATED BY *EGS* SIMULATION

We performed Monte Carlo simulations with the Electron Gamma Shower (*EGS*) simulator to estimate the capability of this instruments. We set geometries and mass elements which are similar to one of figure 2. We also included the satellite body as a scatterer in the geometry as the 1 m × 1 m × 1 m box with 2.65 cm thickness of aluminum which is equivalent to the mass of solar sail (∼ 400 kg).

3.1. Modulation Factor and Efficiency

In figure 6, we show two simulated modulation curves for the monochromatic 100 keV photon with 100 % and 0 % polarization. These photons are uniformly radiated from the front of detector.

We frequently use the modulation factor (M) to indicate the detector sensitivity for the polarization measurement. It is defined as

$$M \equiv \frac{N_{max} - N_{min}}{N_{max} + N_{min}} = \frac{\text{amplitude of } \sin^2\phi}{\text{average of } \sin^2\phi}. \tag{2}$$

For the case of 100 % polarization (large amplitude curve), we estimate the modulation factor of $M = 0.39$. On the other hand, for the non-polarization case (almost constant), the standard deviation of the angular distribution is only 1 % without any rotation of instruments. This fact leads us to conclude the fake modulation from geometric asymmetry is kept under 1 %. Since the dodecagonal shape is very close to the circle, it is very appropriate form as the gamma-ray polarimeter. We also estimate the efficiency (η) which is the ratio of the number of plastic–CsI events to total incoming photons.

Since the total sensitivity for the polarization measurement depends on both M-factor and η, we should evaluate the detector capability with a minimum detectable polarization (MDP) described as;

$$MDP = \frac{\alpha}{M(\eta S)^{1/2}}\sqrt{\frac{\eta F S + B}{T}}, \quad \alpha = 3\sqrt{2} \text{ for 3 sigma confidence.} \tag{3}$$

Here, T is the duration time (in second) of GRBs, F (photon cm^{-2}s^{-1}) and B (photon s^{-1}) denote the source flux and the background count rate, respectively. The parameter $S = 78.5$ (cm^2), for this instrument, means the

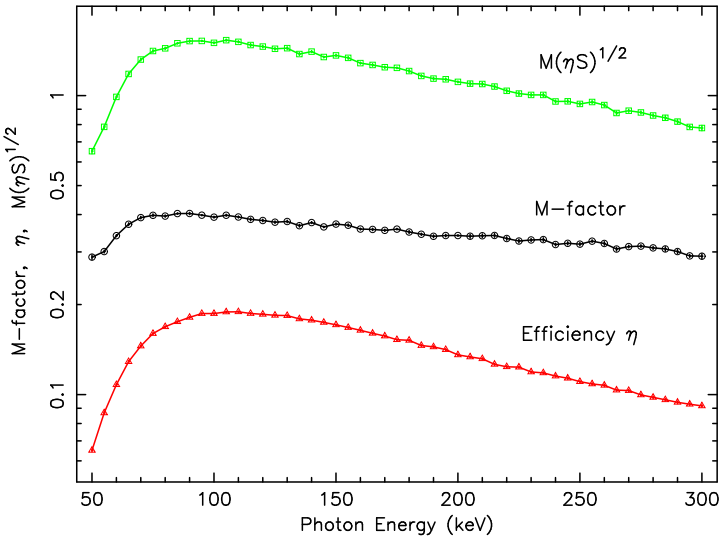

Figure 7. The detector capability obtained by the *EGS* simulations. Each parameter (M-factor, η and $M(\eta S)^{1/2}$) are plotted on the same figure as the function of incoming photon energy. We optimized that the sensitivity of polarization measurement becomes the best around 100 keV which is typical photon energy of GRBs.

effective area. In figure 7, we show the energy dependences of these three parameters M-factor, η and $M(\eta S)^{1/2}$. We design it to optimize the sensitivity has the maximum around 100 keV.

3.2. Diffuse Gamma-Ray Background

The most significant background radiation is the isotropic diffuse gamma-ray. The detector is irradiated by them at all time, and we measure the GRB's polarization in such environments. Therefore, we have to treat the diffuse gamma-ray background when we estimate the detection rate of GRB's polarization. Using the geometrical mass model including the satellite body as described above, we traced the behavior of background radiation. We used the energy spectrum of diffuse gamma-ray as;

$$\frac{dN}{dE} = 167\ E^{-2.38} \quad \text{photon cm}^{-2}\text{s}^{-1}\text{str}^{-1}\text{keV}^{-1}. \tag{4}$$

We notice only the events with the coincidence between plastic and CsI. These background photon without coincidence and with multi-coincidence can be removed, but the plastic–CsI events cannot be distinguished from source signals. Such background radiations contaminate the modulation curves. Using equation 4, integrating 50–300 keV range, we estimate total background flux as $B \sim 32$ photon s^{-1}. Several passes can be considered for plastic–CsI events of background photons; 21 cts s^{-1} is directly into the plastic from the front, 5 cts s^{-1} is from the side CsI (transparent), 6 cts s^{-1} is incoming from back (scattered by the satellite body). We will use passive graded-shields made of Sn and Pb to remove background events. We should consider the charged particle of cosmic-ray. However their energy deposit in scintillators are very large, and signals are rejected by the upper discriminator. Additionally we can distinguish whether the event pattern is single hit, double- or multi-coincidence event.

3.3. Diagonal Response

We carefully designed the polarimeter to give geometrical symmetry for the layout of both plastic and CsI scintillators. As shown in the previous subsection, we succeed to keep the fake modulation down to 1 % level for the non-polarized gamma-ray source. However that is the result for the radiation from the detector normal front. We should estimate the response for the radiation from diagonal position because GRBs occur at random in the field of view.

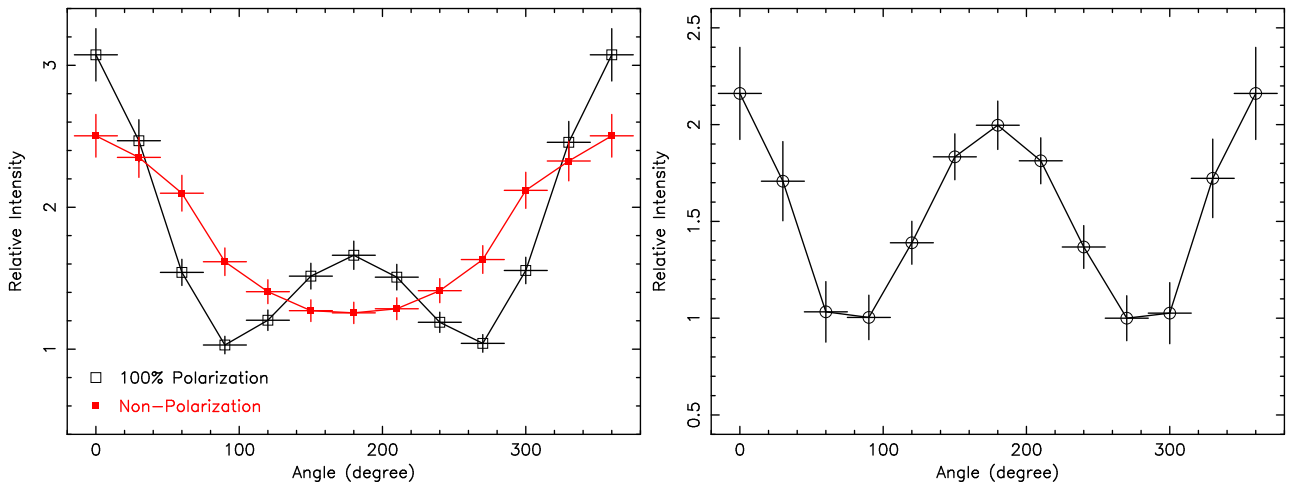

Figure 8. The left panel shows two modulation curves for the radiation with 100 % and 0 % polarization from the diagonal position of 30 degree off-axis. In such case, there is complex fake modulation even if non-polarized photons. The right panel shows the subtracted modulation curves. If we can estimate the modulation curve for the diagonally incoming photon, the source modulation can be extracted.

In figure 8 (left), we show two simulated modulation curves assuming the GRB flux of 10 photon $cm^{-2}s^{-1}$ with the time duration of 20 sec. Each one is the non-polarized and the 100 % polarized case irradiated from 30 degree off-axis. Even if the non-polarized case, there is large fake modulation because the effective area seen from diagonal incidence looks like to the elliptical surface. Then, for the 100 % polarized case, the modulation curve becomes more complicated as shown in figure 8. If we can determine the precious GRB position with the IPN, and estimate the modulation curves for non-polarized case by simulations, we can obtain the real modulation curves to subtract background modulation from observed modulation curves as shown in figure 8 (right).

3.4. Detection Probability

Considering the detector sensitivity discussed above, we estimate the detection rate for GRB's polarization based on the past GRB detector, *BATSE*, aboard the *Compton Gamma-Ray Observatory*. According to *BATSE* catalog, 2704 GRBs were detected in the mission time of 9 years. Since an average fraction of the sky coverage of *BATSE* is 0.483, the GRB rate is 49.5 events $yr^{-1}str^{-1}$. Using the flux and the duration time, we estimate the *MDP* for each GRB from equation 3 in the circumstance of the background count rate $B = 32$ Hz. In figure 9, we show the GRB occurring rate within our field of view as the function of *MDP*. In the figure, two cases are plotted at once. One is the case for whole FOV, and another is within the central 30 degrees. If the prompt emissions of GRBs have the polarization degree of 50 %, we have several chance to observe them. A few events occur in close to the central optical axis, so we may enable to detect their polarization above 3 σ confidence level in the condition of little (removable) fake modulation.

4. CONCLUSIONS

We will mount the dodecagonal gamma-ray polarimeter aboard the solar powered sail satellite planed to launch in 2012. The aim of this instrument is to detect the polarization degree of the prompt GRBs. The detector sensitivity is the modulation factor $M = 0.39$, the efficiency $\eta = 0.2$, and the minimum detectable polarization $M(\eta S)^{1/2} = 1.55$. The detection rate of GRB's polarization is expected to be a few events per year which occur in the central part of FOV with the half angle of 30 degrees.

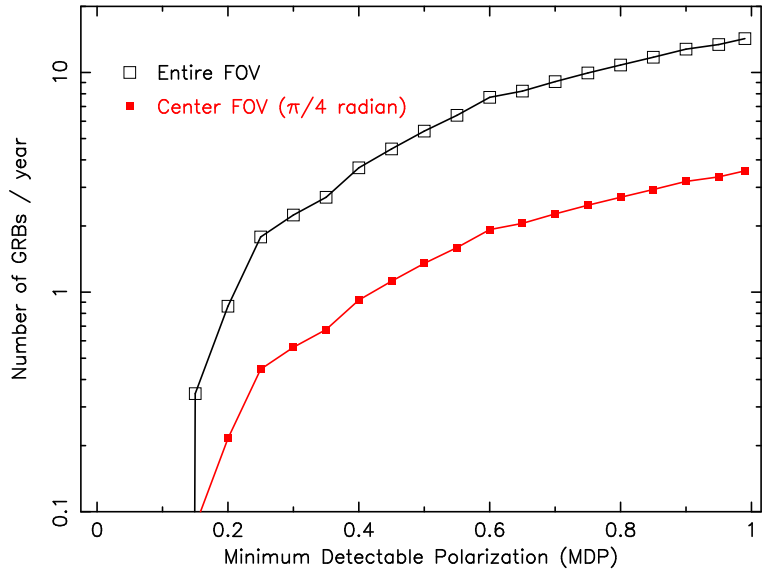

Figure 9. The detection rate of the GRB's polarization as the function of MDP. The open and close square indicate the GRB rate within the entire and the central (30 degree of the half angle : $\pi/4$ radian) field of view. A few events per year is expected to succeed the polarization measurement if the prompt emissions have the polarization degree of 50 %.

REFERENCES

1. *Clear Pulse Home Page, http://www.clearpulse.co.jp/files/top-e.html*
2. W. Coburn & S. E. Boggs, *Polarization of the prompt γ-ray emission from the γ-ray burst of 6 December 2002*, Nature, 423, 415, 2003.
3. E. Costa, F. Frontera, J. Heise et al. *Discovery of an X-ray afterglow associated with the gamma-ray burst of 28 February 1997*, Nature, 387, 783, 1997.
4. S. Gunji, H. Sakurai, M. Noma, E. Takase T. Saito & H. Misawa *A New Design of Hard X-Ray Polarimeter*, IEEE Transactions on Nuclear Science, 41, No.4, 1994
5. S. Gunji, E. Kudo & H. Sakurai *Improvement of the Modulation Factor for a Compton Scattering Type Polarimeter Using Subdivided Scintillators*, IEEE Conf. Rec. 1997
6. S. Gunji, T. Suzuki, F. Sato, H. Sakurai, F. Tokanai, Y. Saito & A. Kubota *Development of hard X-ray polarimeter for gamma-ray bursts*, Advanced Space Research, 33, 1771, 2004
7. *Hamamatsu Photonics Home Page, http://jp.hamamatsu.com/en/index.html*
8. K. Hayashida, T. Mihara, S. Gunji, F. Tokanai, *Hard X-ray polarimeter for small satellite: design, feasibility study, and ground experiments*, SPIE, 5501, 44, 2004.
9. J. Kataoka, et al., *Low energy response of a prototype detector array for the PoGO astronomical hard x-ray polarimeter*, SPIE, 5898, 133, 2005.
10. T. Mihara, & H. Miyamoto, *Octagonal Scintillator for Hard X-ray Polarimetry*, X-ray Polarimetry Workshop, SLAC, Stanford, USA., 2004.
11. *OSO-8 Home Page, http://heasarc.gsfc.nasa.gov/docs/oso8/oso8.html*
12. E. Takase, S. Gunji, H. Sakurai, M. Noma, H. Tomita, F. Denzumi & T. Tamura *Development of a new hard X-ray polarimeter*, SPIE, 2283, 265, 1994
13. *ISAS/JAXA Home Page, http://www.isas.ac.jp/j/special/2005/plan/03.shtml*
14. T. Suzuki, S. Gunji, R. Nakajima, Y. Yamashita, K. Suzuki, H. Sakurai, F. Tokanai, K. Takashima, Y. Kobayashi, K. Tamura & S. Kitamoto *Performance of Prototype Hard X-ray Polarimeter Utilizing Compton Scattering*, Japanese Journal of Applied Physics, 45, No. 1, 2006